3954 J. Med. Chem. 2010, 53, 3954–3963
DOI: 10.1021/jm901785w

Journal of Medicinal Chemistry Article

Novel N^2-Substituted Pyrazolo[3,4-*d*]pyrimidine Adenosine A_3 Receptor Antagonists: Inhibition of A_3-Mediated Human Glioblastoma Cell Proliferation†

Sabrina Taliani,‡ Concettina La Motta,*,‡ Laura Mugnaini,‡ Francesca Simorini,‡ Silvia Salerno,‡ Anna Maria Marini,‡ Federico Da Settimo,‡ Sandro Cosconati,§ Barbara Cosimelli,§ Giovanni Greco,§ Vittorio Limongelli,§ Luciana Marinelli,§ Ettore Novellino,§ Osele Ciampi,∥ Simona Daniele,∥ Maria Letizia Trincavelli,∥ and Claudia Martini∥

‡*Dipartimento di Scienze Farmaceutiche, Università di Pisa, Via Bonanno 6, 56126 Pisa, Italy,* §*Dipartimento di Chimica Farmaceutica e Tossicologica, Università di Napoli "Federico II", Via D. Montesano 49, 80131 Napoli, Italy, and* ∥*Dipartimento di Psichiatria, Neurobiologia, Farmacologia e Biotecnologie, Università di Pisa, Via Bonanno 6, 56126 Pisa, Italy*

Received December 2, 2009

Adenosine induces glioma cell proliferation by means of an antiapoptotic effect, which is blocked by cotreatment with selective A_3 AR antagonists. In this study, a novel series of N^2-substituted pyrazolo-[3,4-*d*]pyrimidines **2a**−**u** was developed as highly potent and selective A_3 AR antagonists. The most performing compounds were derivatives **2a** (R_1 = CH_3 and R_2 = COC_6H_5; K_i 334, 728, and 0.60 nM at the human A_1, A_{2A}, and A_3 ARs, respectively) and **2b** (R_1 = CH_3 and R_2 = COC_6H_4-4-OCH_3; K_i 1037, 3179, and 0.18 nM at the human A_1, A_{2A}, and A_3 ARs, respectively), which counteracted the effect of the A_3 AR agonists Cl-IB-MECA and IB-MECA on human glioma U87MG cell proliferation. This effect was concentration-dependent, with IC_{50} values comparable to A_3 AR binding affinity values of **2a** and **2b**, thereby suggesting that their effects were receptor-mediated. Furthermore, the antiproliferative activity of the new compounds was demonstrated to be mediated by the block of A_3 AR agonist activation of intracellular kinases ERK 1/2.

Introduction

Adenosine is an endogenous purine nucleoside that modulates a wide variety of physiological actions by triggering specific cell membrane G-protein-coupled receptors (GPCRs[a]). Adenosine receptors (ARs) are widely distributed in mammalian tissues and have been classified into the four following subclasses: A_1, A_{2A}, A_{2B}, and A_3.[1−3]

The adenosine A_1 and A_3 ARs are coupled to the G_i protein, which inhibits adenylate cyclase. In contrast, the A_{2A} and A_{2B} ARs stimulate adenylate cyclase via a G_s protein. Additional couplings to other second messenger systems have been described, including the stimulation of phospholipase C (A_1, A_{2B}, and A_3) as well as the activation and inhibition of potassium and calcium channels, (A_1) respectively.[4]

ARs are currently of great interest as targets for therapeutic intervention in many pathological conditions such as renal failure, cardiac and cerebral ischemia, central nervous system (CNS) disorders, neurodegenerative diseases, and inflammatory pathologies such as asthma.[5,6] Indeed, the development of potent and selective synthetic AR antagonists has been the subject of medicinal chemistry research for more than three decades.[5,6]

The A_3 AR is widely distributed in peripheral organs and is found in high levels in the testis and in lower levels in the lung, kidney, and heart as well as in regions of the CNS.[7] The A_3 AR is involved in a variety of important physiological processes, including modulation of cerebral and cardiac ischemic damage,[8−10] inflammation,[11] modulation of intraocular pressure,[12] regulation of normal and tumor cell growth,[13−15] and immunosuppression.[16] Consequently, A_3 AR selective antagonists have been proposed as novel anti-inflammatory drugs, as cerebroprotective agents for preventing ischemic brain damage, and as new agents for the treatment of glaucoma.[16] Furthermore, the significant overexpression of A_3 AR in several types of tumor cells,[17] together with the pro-survival and antiapoptotic effects of A_3 AR stimulation, has recently led Baraldi et al. to propose that antagonists at this receptor might sensitize tumor cells to chemotherapeutic drugs.[14,18] In this regard, recent studies have shown that the specific A_3 AR antagonist MRS1220 blocked adenosine-mediated glioma cell proliferation, thereby suggesting that A_3 AR antagonists are possible adjuvant agents in glioma chemotherapy.[19] Recently, it has been demonstrated that extracellular regulated kinases (ERK 1/2), as well as p38 and Akt kinases, are intracellular phosphorylative pathways involved in A_3 AR-mediated proliferative effects in glioblastoma cell lines.[20]

Our research group has developed several classes of A_1 and A_3 AR antagonists,[21−26] including the imidazo[1,2-*a*][1,3,5]triazines **1** (Chart 1).[22,23] Among this series, derivative **1a** (Chart 1, R_1 = CH_3 and R_2 = COPh) exhibited the highest potency at the A_3 AR and demonstrated fair selectivity for A_3 over the A_1 and A_{2A}

†This paper is dedicated to Prof. Fulvio Gualtieri on the occasion of his retirement.

*To whom correspondence should be addressed. Phone: +390502219593. Fax: +390502219605. E-mail: lamotta@farm.unipi.it.

[a] Abbreviations: AB-MECA, 4-aminobenzyl-5′-*N*-methyl-carboxamidoadenosine; ADA, adenosine deaminase; AR, adenosine receptor; Cl-IB-MECA, 2-chloro-N^6-(3-iodobenzyl)adenosine-5′-*N*-methylcarboxamide; DPCPX, 8-cyclopentyl-1,3-dipropylxanthine; EHNA, *erythro*-9-(2-hydroxy-3-nonyl)adenine; ERK 1/2, extracellular regulated kinase 1 and 2; GPCRs, G-protein-coupled receptors; IB-MECA, N^6-(3-iodobenzyl)-adenosine-5′-*N*-methylcarboxamide; NECA, adenosine-5′-(*N*-ethylcarboxamide); SEM, standard error of mean.

 Published on Web 04/21/2010

ARs (K_i values measured on human A_3, A_1, and A_{2A} ARs were 3 nM, 350 nM, and $>10\ \mu$M, respectively).[22,23]

Furthermore, we have recently reported a series of pyrazolo[3,4-*d*]pyrimidines **2** (Chart 1) that act as adenosine deaminase (ADA) inhibitors,[27,28] which are isosterically related to imidazo[1,2-*a*][1,3,5]triazines **1**. The most active compound of series **2** was found to be effective at reducing systemic and intestinal inflammatory alterations in an experimental model of colitis.[28]

As a logical extension of these projects, we designed novel N^2-substituted pyrazolo[3,4-*d*]pyrimidine derivatives of series **2** as A_3 AR antagonists. Indeed, a large number of AR antagonists featuring the pyrazolo[3,4-*d*]pyrimidine scaffold have been reported, but all of them have been N^1-substituted and have shown a high affinity and selectivity for the A_1 or A_{2A} ARs.[29−31]

In almost all the new compounds **2**, the 6 position of the bicyclic scaffold possesses a phenyl ring in consideration of its pharmacophoric role as evidenced in the AR antagonist series **1**[22] and of its unfavorable effect on ADA inhibitory activity.[27] Substituents at the 2 position were represented by a methyl group, in analogy to the lead compound **1a**, or by a phenylalkyl group known to be detrimental to ADA inhibitory activity. Finally, the R^2 substituents attached to the exocyclic N^4 were selected by taking into account literature data about the key role of NH-acyl side chains in ligand recognition by the A_3 AR.[32−36]

The present paper describes the synthesis, the biological evaluation, and the molecular modeling studies of a number of pyrazolo[3,4-*d*]pyrimidines **2a**−**u** as A_3 AR antagonists. Two of the best performing new compounds, **2a** and **2b**, were evaluated for their inhibitory activity on the A_3 AR-mediated glioma cell proliferation.

Chart 1. Structures of Known (**1**) and New (**2**) A_3 AR Antagonists

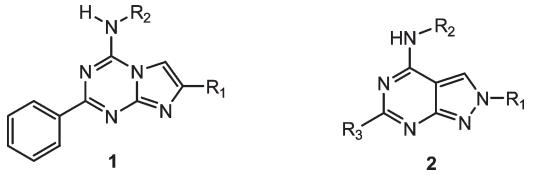

Chemistry

The synthesis of the target compounds **2a**−**u** was performed as outlined in Scheme 1. The 3-amino-N^1-substituted-4-pyrazolecarbonitriles **3**−**5** were cyclized to the corresponding 6-phenylpyrazole[3,4-*d*]pyrimidines **6**−**8** through a reaction with benzonitrile in the presence of potassium *tert*-butoxide and under microwave irradiation according to our previously published procedure.[27] Cyclization of **4** with boiling formamide provided the 6-unsubstituted pyrazolo[3,4-*d*]pyrimidine **9**.[27]

The key intermediates **6**−**9** yielded the N^4-aroyl compounds **2a**−**c**, **2g**−**i**, **2m**−**o**, and **2s**−**u** by reaction with the suitable aroylchloride in the presence of triethylamine. These same intermediates also yielded the N^4-carbamoyl derivatives **2d**−**f**, **2j**−**l**, and **2p**−**r** by treatment with the appropriate isocyanate. Both procedures were carried out under microwave irradiation (Scheme 1).

Biology

The affinities of the new compounds toward human A_1, A_{2A}, and A_3 ARs were evaluated by competition experiments by assessing their respective abilities to displace [^{3}H]DPCPX, [^{3}H]NECA, or [^{125}I]AB-MECA binding from

Scheme 1. Synthesis of Target Compounds **2a**−**u**[a]

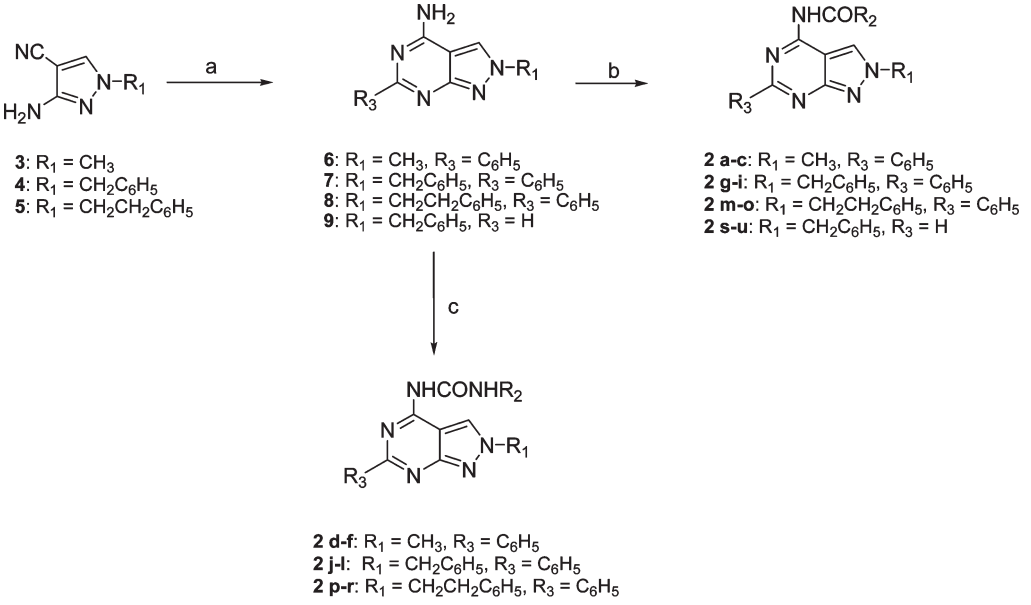

R_2	compd
C_6H_5	**2a, 2d, 2g, 2j, 2m, 2p, 2s**
C_6H_4-4-OCH_3	**2b, 2e, 2h, 2k, 2n, 2q, 2t**
C_6H_4-3-Cl	**2c, 2f, 2i, 2l, 2o, 2r, 2u**

[a] Reaction conditions: (a) benzonitrile, *t*-BuOK, MW, or boiling formamide, 12 h;[26] (b) substituted-benzoylchloride, NEt_3, MW; (c) substituted-phenylisocyanate, MW.

Table 1. Binding Affinity at Human A_1, A_{2A}, and A_3 ARs of 2-Substituted-pyrazolo[3,4-*d*]pyrimidine derivatives **6**−**8** and **2a**−**u**

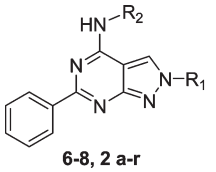

6-8, 2 a-r

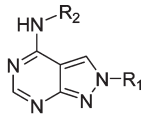

2 s-u

			K_i (nM)[a]		
no.	R_1	R_2	hA_1[b]	hA_{2A}[c]	hA_3[d]
6	CH_3	H	584.7 ± 57.0	> 10000	922.0 ± 19.0
2a	CH_3	COC_6H_5	334.0 ± 32.0	728.1 ± 70.3	0.60 ± 0.10
2b	CH_3	COC_6H_4-4-OCH_3	1037.0 ± 105.0	3179.0 ± 315.0	0.18 ± 0.02
2c	CH_3	COC_6H_4-3-Cl	1081.6 ± 110.0	886.0 ± 42.0	5.9 ± 0.9
2d	CH_3	$CONHC_6H_5$	> 10000	> 10000	20.9 ± 1.2
2e	CH_3	$CONHC_6H_4$-4-OCH_3	> 10000	> 10000	357.9 ± 35.8
2f	CH_3	$CONHC_6H_4$-3-Cl	> 10000	> 10000	29.1 ± 2.4
7	CH_2-C_6H_5	H	312.0 ± 11.0	121.1 ± 1.0	93.0 ± 5.0
2g	CH_2-C_6H_5	COC_6H_5	53.0 ± 1.1	180.6 ± 1.7	3.0 ± 0.1
2h	CH_2-C_6H_5	COC_6H_4-4-OCH_3	> 10000	> 10000	22.1 ± 2.4
2i	CH_2-C_6H_5	COC_6H_4-3-Cl	> 10000	> 10000	3.7 ± 0.3
2j	CH_2-C_6H_5	$CONHC_6H_5$	290.0 ± 11.0	> 10000	2.9 ± 0.5
2k	CH_2-C_6H_5	$CONHC_6H_4$-4-OCH_3	> 10000	> 10000	2.9 ± 0.1
2l	CH_2-C_6H_5	$CONHC_6H_4$-3-Cl	> 10000	> 10000	120.8 ± 11.3
8	CH_2CH_2-C_6H_5	H	2500.0 ± 170.0	1000.0 ± 200.0	503 ± 17
2m	CH_2CH_2-C_6H_5	COC_6H_5	27.0 ± 6.1	227.0 ± 12.0	43.7 ± 2.4
2n	CH_2CH_2-C_6H_5	COC_6H_4-4-OCH_3	2400.0 ± 110.0	1136.0 ± 95.0	45.2 ± 5.3
2o	CH_2CH_2-C_6H_5	COC_6H_4-3-Cl	1050.0 ± 99.0	314.0 ± 22.0	22.3 ± 1.3
2p	CH_2CH_2-C_6H_5	$CONHC_6H_5$	1700.0 ± 123.0	96.0 ± 6.1	36.3 ± 2.1
2q	CH_2CH_2-C_6H_5	$CONHC_6H_4$-4-OCH_3	> 10000	> 10000	> 1000
2r	CH_2CH_2-C_6H_5	$CONHC_6H_4$-3-Cl	> 10000	> 10000	> 1000
2s	CH_2-C_6H_5	COC_6H_5	> 10000	> 10000	> 1000
2t	CH_2-C_6H_5	COC_6H_4-4-OCH_3	> 10000	> 10000	> 1000
2u	CH_2-C_6H_5	COC_6H_4-3-Cl	> 10000	4900.0 ± 360.0	> 1000
DPCPX			3.9	130	4000
NECA			14.0	20	6.2
Cl-IBMECA			120	2100	11

[a] The K_i values are means ± SEM derived from an iterative curve-fitting procedure (Prism program, GraphPad, San Diego, CA). [b] Displacement of specific [^{3}H]DPCPX binding in membranes obtained from hA_1 AR stably expressed in CHO cells. [c] Displacement of specific [^{3}H]NECA binding in membranes obtained from hA_{2A} AR stably expressed in CHO cells. [d] Displacement of specific [^{125}I]AB-MECA binding in membranes obtained from hA_3 AR stably expressed in CHO cells.

transfected CHO cells. Experiments were performed as described previously.[23] Compounds **2a**, **2b**, **2g**, and **2i**−**k**, which showed a high A_3 AR affinity, were tested in functional assays at human A_{2B} and A_3 ARs by measuring their effects on NECA-mediated cAMP modulation in transfected CHO cells.[37]

Compounds **6**−**8**, **2a**−**g**, and **2i**−**k** were also evaluated for their inhibitory activity against bovine spleen ADA using (+)-EHNA as the reference standard, as previously reported.[27]

Compounds **2a** and **2b** were tested for their effect on the proliferation of U87MG human glioma cells. U87MG cells, which were blocked in G1 phase, were treated with the A_3 AR agonists Cl-IB-MECA or IB-MECA in the absence or in the presence of compounds **2a** or **2b** for 48 h. At the end of this period, the number of living cells was determined by the Trypan blue exclusion test. In this assay, cells with a damaged cell membrane stain blue, while cells that maintain plasma membrane integrity resist dye entry and remain unstained (apoptotic and healthy cells, respectively). Finally, the effects of the new compounds on A_3 AR-mediated activation of intracellular ERK 1/2 were evaluated by incubating U87MG cells with Cl-IB-MECA in the presence of different **2a** or **2b** compound concentrations. Following 30 min cell incubation, the phosphorylated ERK 1/2 levels were quantified using an ELISA kit.

Results and Discussion

Table 1 lists the binding affinities at the human A_1, A_{2A}, and A_3 ARs of the newly synthesized 2-substituted pyrazolo[3,4-*d*]-pyrimidines **2a**−**u** expressed as K_i values. The intermediate products **6**−**8**, which were also assayed, exhibited moderate potency and selectivity for the A_3 AR, and no ADA inhibitory activity at 10 μM concentration (data not shown).

Within the set of 2-methyl derivatives (R_1 = CH_3), the introduction of a benzoyl group attached to the N^4 of **6** yielded **2a** (R_2 = COC_6H_5), **2b** (R_2 = COC_6H_4-4-OCH_3), and **2c** (R_2 = COC_6H_4-3-Cl) and dramatically increased the potency and selectivity at the A_3 AR. Among the above NH-acyl derivatives, **2b** stood out as a subnanomolar A_3 AR antagonist with micromolar affinity at the A_1 and A_{2A} ARs.

Replacement of the benzoylamino moiety of **2a**−**c** with a phenylcarbamoyl moiety to give **2d**−**f** lowered the affinity to all the ARs.

None of the 2-benzyl derivatives (R_1 = CH_2-C_6H_5) was more potent at the A_3 AR than the 2-methyl derivative **2b**. Generally, the structure−affinity relationships (SARs) within the set of 2-benzyl derivatives **7**, **2g**−**l** did not exactly parallel those of the 2-methyl derivatives **6**, **2a**−**f**. As an example, the $CONHC_6H_4$-4-OCH_3 chain attached to N^4 gave the best and

Table 2. Potency of Compounds **2a**, **2b**, **2g**, and **2i**−**k** versus hA_{2B} and hA_3 Adenosine Receptor Subtypes

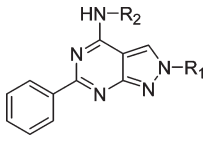

			IC_{50} (nM) in cAMP assays[a]	
no.	R_1	R_2	hA_{2B} CHO cells	hA_3 CHO cells
2a	CH_3	COC_6H_5	49.8 ± 2.8	1.9 ± 0.1
2b	CH_3	COC_6H_4-4-OCH_3	53.9 ± 5.9	2.4 ± 0.2
2g	CH_2-C_6H_5	COC_6H_5	272.0 ± 25.0	53.0 ± 4.3
2i	CH_2-C_6H_5	COC_6H_4-3-Cl	1327.0 ± 137.0	7.6 ± 0.7
2j	CH_2-C_6H_5	$CONHC_6H_5$	1324.0 ± 130.0	5.7 ± 0.6
2k	CH_2-C_6H_5	$CONHC_6H_4$-4-OCH_3	1467.0 ± 130.0	8.2 ± 0.8

[a] The data are expressed as the mean ± SEM of four independent experiments performed in triplicate.

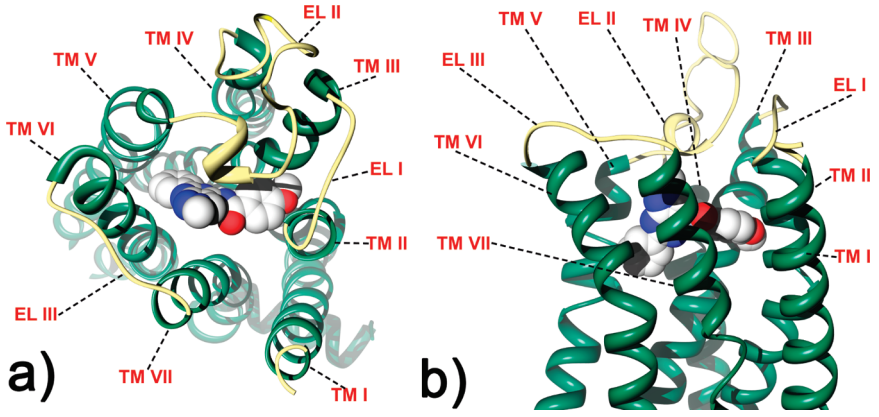

Figure 1. Top (a) and front (b) view of the **2b**/hA_3 AR complex.

the worst results in the series of 2-benzyl (**2k**) and 2-methyl (**2e**) derivatives, respectively.

Replacement of the 2-benzyl group of **7**, **2g**−**l**, with a 2-phenylethyl moiety to give the corresponding homologues **8**, **2m**−**r** produced a general decrease in A_3 AR affinity, probably due to unfavorable steric effects, and different effects on the binding for the A_1 and A_{2A} ARs.

Finally, the poor affinity of compounds **2s**−**u** for all the ARs suggests that the 6-phenyl substituent is a key pharmacophoric element for the recognition of our pyrazolo[3,4-*d*]-pyrimidines with each of these receptors.

Compounds **2a**, **2b**, **2g**, and **2i**−**k** were also tested at the A_{2B} AR by evaluating their inhibitory effects on NECA-mediated cAMP accumulation in CHO cells stably expressing this receptor subtype (Table 2). Interestingly, the N^2-methyl derivatives **2a** and **2b** displayed a nanomolar activity in this assay even though maintaining a good selectivity for the A_3 AR. These products may represent promising lead compounds for the development of potent and selective A_{2B} AR antagonists featuring the 2-substituted-pyrazolo[3,4-*d*]pyrimidine scaffold. Conversely, the other selected derivatives **2g** and **2i**−**k** showed submicromolar/micromolar IC_{50} values, thereby indicating a poor to moderate affinity toward the A_{2B} AR.

Given the recent discoveries regarding non-nucleoside AR agonists,[38,39] the efficacy profiles of **2a**, **2b**, **2g**, and **2i**−**k** were evaluated in cAMP functional assays at the A_3 AR (Table 2). As expected, all of these compounds displayed full antagonism with potencies similar to their binding affinity. Furthermore, when tested in the absence of NECA, they did not show any significant effect on the cAMP level even after stimulation by forskolin, thereby indicating neutral antagonism (data not shown).

Finally, compounds **2a**−**g** and **2i**−**k** were also evaluated for their inhibitory activity against bovine spleen ADA using (+)-EHNA as the reference standard, as previously reported.[27] Notably, all of the compounds tested displayed no appreciable inhibitory activity at 10 μM concentration (data not shown).

Molecular modeling studies were undertaken to rationalize the SARs regarding the binding of compounds **2a**−**u** to the A_3 AR.

A homology model of the human A_3 AR was constructed using as a template the recently published crystal structure of the human A_{2A} AR (PDB code 3EML).[40]

The sequence alignment between the two receptors and the positions of the disulfide bridges were attained consistently with what was already suggested by Moro and co-workers.[41] The structure of the A_3 AR was then used to perform docking calculations on **2b**, **2i**, **2o**, and **2t** employing the software AudoDock4 (AD4).[42] The obtained docking poses were evaluated for their consistency with the available SARs as well as for the calculated binding free energy (ΔG_{AD4}).

The docking results achieved for **2b** revealed that this ligand binds to the outer portion of the A_3 AR being surrounded by TMs III, V, VI,VII helices and ELII (Figure 1a,b). More precisely, its methyl group (R_1) points to the outer part of the receptor taking contact with the side chains of F168 and L246 belonging to the ELII, its aroyl chain (R_2) is embedded in the fissure between TMII and TMIII, and its pendant 6-phenyl ring is oriented toward the inner portions of TMV and TMVI.

As depicted in Figure 2, this binding pose allows the pyrazolopyrimidine scaffold of **2b** to engage a π-stacking interaction with the F168 side chain and two H-bonds between its N1 and N7 nitrogens and the N250 side chain. Interestingly, the latter residue was found to be critical for ligand binding at both the A_3 and A_{2A} ARs.[43,44] Moreover, the 6-phenyl ring of the ligand is embedded in a hydrophobic cleft formed by I186, L91, W243, L246, and S247. Among these residues, W243 was considered to play a crucial role in receptor activation and antagonist binding.[44] Additionally, the aroyl moiety is located in a lipophilic pocket, at the interface between TMII and TMIII, made up by L68, A69, V72, T87, and L89. The tight interaction of this group with the receptor might explain why the nature of the R_2 substituent affects so strongly the potency at the A_3 AR (see K_i values of **6** and **2a**−**f**).

According to our docking calculations, **2i** is oriented differently from **2b** at the A_3 AR. In particular, its aroyl chain (R_2) points to the extracellular portion of the receptor taking favorable contacts with the EL2 region, while its benzyl group (R_1) is located within the lipophilic cleft at the crevice between TMII and TMIII (Figure 3a). The above differences might explain why for **7** and **2g**−**l** the bulkiness of the R_2 substituent (which now points to the roomier extracellular region) influences affinity to the A_3 AR to a lower extent compared with what happens for **6** and **2a**−**f**. The orientation of the pyrazolopyrimidine system of **2i** within the A_3 AR still allows a double H-bond with N250 and a tight interaction of the pendant 6-phenyl ring with W243.

The docking results achieved for **2o** indicate that the binding pose of this ligand (Figure 3b) is roughly similar to that of **2i** (Figure 3a). However, for steric reasons, the phenylethyl moiety of **2o** is oriented outward the lipophilic cleft hosting the benzyl chain of **2i**. This difference is consistent with the drop of affinity to the A_3 AR associated with the replacement of the benzyl with the phenylethyl substituent.

Docking calculations on **2u** were performed to rationalize the lack of affinity to the A_3 AR characterizing all the compounds devoid of the 6-phenyl ring (**2s**−**u**). The binding pose of **2u** (Figure 4) resembles that of **2b**, as both molecules orient the R_1 and the R_2 substituents in the same receptor regions. As expected, the absence of the 6-phenyl ring in the structure of **2u** implies the loss of crucial interactions with the W243 side chain.

To estimate the drugability of compounds **2a** and **2b**, provided with the best affinity and selectivity at the A_3 AR, we calculated some of their physicochemical properties, namely log *P*, ASA, PSA, the number of H-bond donors and acceptors, the number of atoms and bonds, the number of rotatable bonds, and the molecular weight (Table 3).[45] These data suggest that **2a** and **2b** display a drug-like character and that basically fulfill the physicochemical requirements for an adequate distribution into the CNS.

Prompted by these results, we investigated the effects of **2a** and **2b** on proliferation of the U87MG human glioblastoma cell line.

In U87MG cells, the A_3 agonists Cl-IB-MECA (100 nM) and IB-MECA (12 nM) were able to stimulate cell proliferation. Compounds **2a** and **2b** counteracted the effects of both agonists, Cl-IB-MECA and IB-MECA, with IC_{50} values in the subnanomolar range, comparable to the affinity of these compounds toward A_3 AR (Figure 5). These results suggest that the effects of **2a** and **2b** on cell proliferation may be ascribed to their selective interaction with A_3 AR subtype. Furthermore, the compounds alone did not modulate glioma cell proliferation at the tested concentrations (data not shown), thereby demonstrating that they behave as A_3 AR antagonists.

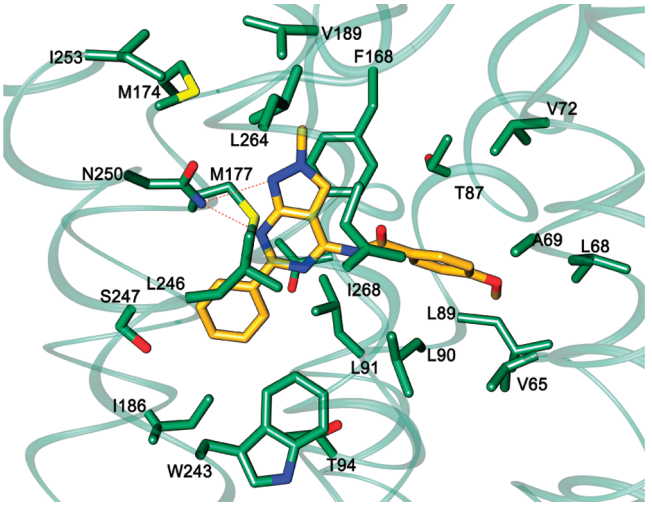

Figure 2. Calculated binding pose for **2b** in the hA_3 AR model.

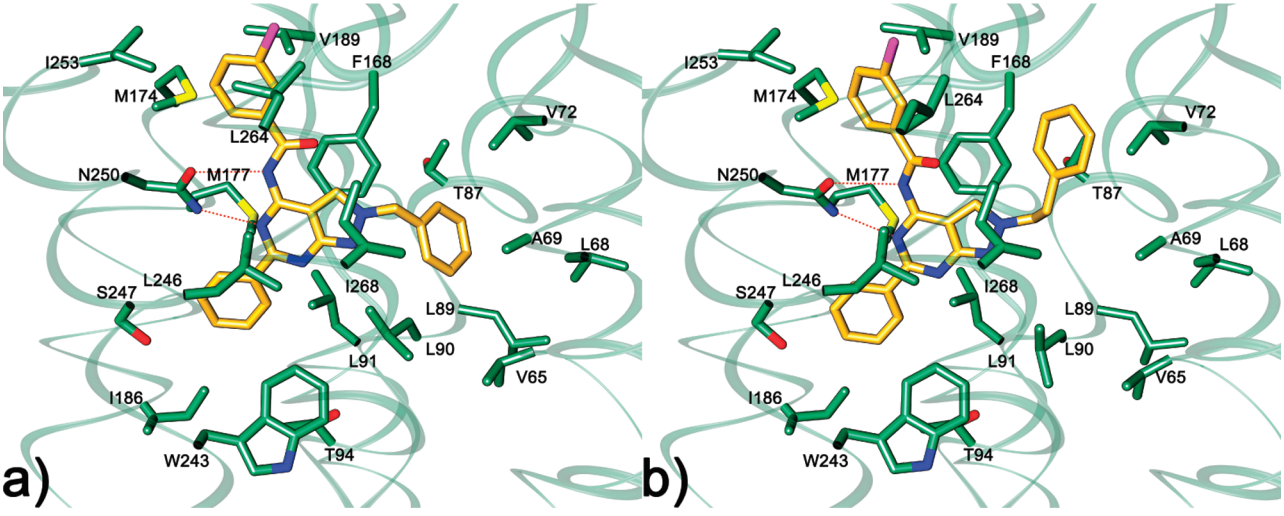

Figure 3. Calculated binding pose for **2i** (a) and **2o** (b) in the hA_3 AR model.

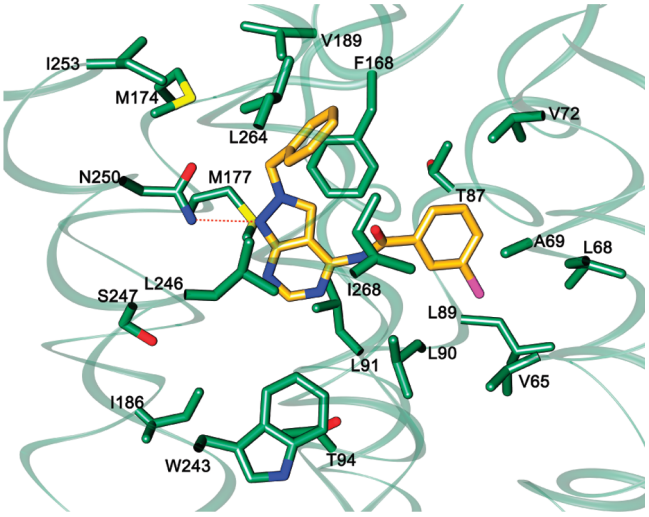

Figure 4. Calculated binding pose for **2u** in the hA_3 AR model.

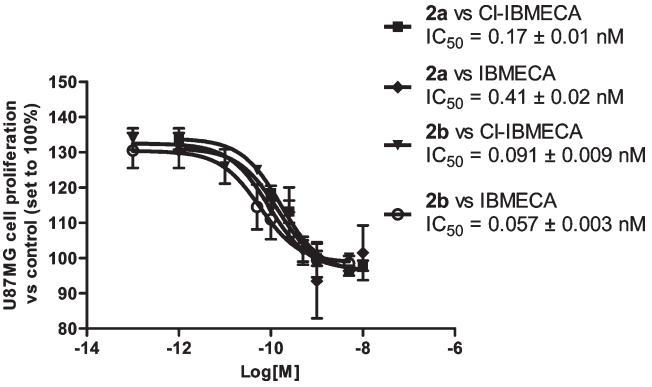

Figure 5. Effect of **2a** and **2b** compounds on Cl-IB-MECA or IB-MECA-induced U87MG cell proliferation. Cells were treated for 48 h with Cl-IB-MECA (100 nM) or IB-MECA (12 nM) in the absence or in the presence of compound **2a** (0.1−10 nM) and **2b** (0.01−5 nM). Live cell counting was determined by using the trypan blue exclusion test. Data (mean ± SEM) were expressed as percentage of living cells with respect to control cells (set to 100%).

Table 3. Physicochemical Predicted Properties of Compounds **2a**, **2b**[45]

	2a	**2b**
log P^a	3.8	4.0
ASA (Å^2)^b	675.4	609.0
TPSA (Å^2)^c	69.0	59.8
donor sites	1	1
acceptor sites	4	3
atom count	45	41
bond count	48	44
rotatable bond count	4	3
molecular weight	359.38	329.36

[a] Calculated *n*-octanol/water partition coefficient. [b] Calculated accessible solvent area. [c] Topological polar surface area.

To explore the intracellular phosphorylative pathways involved in A_3-mediated proliferative effects, the ability of the agonist Cl-IB-MECA (100 nM) to stimulate ERK 1/2 phosphorylation was investigated. The results, depicted in Figure 6, demonstrated that Cl-IB-MECA induced a time-dependent stimulation of ERK 1/2 phosphorylation with a maximum after 30 min of cell incubation. The compounds **2a** and **2b** counteracted the Cl-IB-MECA-mediated activation of ERK 1/2 with a potency corresponding to their affinity

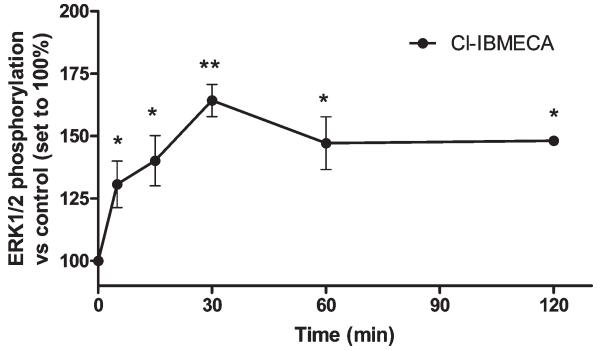

Figure 6. Kinetic of A_3 AR-mediated ERK 1/2 phosphorylation. U87MG cells were treated for different times (5−120 min) with 100 nM Cl-IB-MECA and then ERK 1/2 phosphorylation levels were quantified by Fast Activated Cell-Based ELISA kits. Data (mean ± SEM) were expressed as percentage of phosphorylated ERK 1/2 with respect to control cells (set to 100%). *P < 0.05 vs control; **P < 0.01 vs control, Student t test.

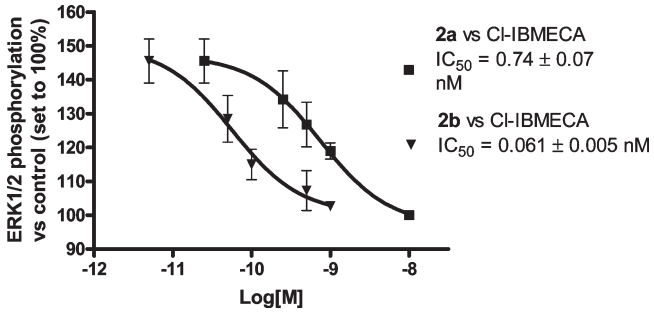

Figure 7. Effect of **2a** and **2b** compounds on Cl-IB-MECA induced ERK 1/2 phosphorylation in U87MG cells. U87MG cells were treated for 30 min with 100 nM Cl-IB-MECA in the absence or in the presence of compound **2a** (0.25−10 nM) and **2b** (0.05−1 nM). ERK 1/2 phosphorylation levels were quantified by Fast Activated Cell-Based ELISA kits. Data (mean ± SEM) were expressed as percentage of phosphorylated ERK 1/2 with respect to control cells (set to 100%).

constant values for A_3 AR (Figure 7). Furthermore, the compounds alone did not modulate ERK 1/2 activation state at the tested concentrations (data not shown), thereby demonstrating that they behave as A_3 AR antagonists. These results demonstrated that A_3 AR induced U87MG cell proliferation occurred through the recruitment of ERK as intracellular phosphorylative pathway.

Conclusions

A number of pyrazolo[3,4-*d*]pyrimidines with the general formula **2** were developed as A_3 AR antagonists with high potency and selectivity. These compounds were designed by taking the imidazo[1,2-*a*][1,3,5]triazine **1a** (Chart 1, R_1 = CH_3 and R_2 = COPh) as a reference structure[22,23] and utilizing our experience in the preparation of pyrazolo[3,4-*d*]pyrimidines as ADA inhibitors.[27,28] The main SARs were substantiated by docking studies performed by means of a hA_3 AR model constructed using as a template the recently published crystal structure of the hA_{2A} AR. The highest affinity and selectivity toward the A_3 AR were exhibited by the N^2-methyl derivatives **2a** (R_1 = CH_3 and R_2 = COC_6H_5; K_i 334, 728, and 0.60 nM at the human A_1, A_{2A}, and A_3 ARs, respectively) and **2b** (R_1 = CH_3 and R_2 = COC_6H_4-4-OCH_3; K_i 1037, 3179, and 0.18 nM at the human A_1, A_{2A}, and A_3 ARs, respectively), which showed

no appreciable ADA inhibitory activity. Both compounds, when tested on human glioma U87MG cells, counteracted the A_3 AR agonists Cl-IB-MECA- and IB-MECA-mediated proliferation through the inhibition of A_3 AR agonist-mediated ERK 1/2 activation. Furthermore, the IC_{50} values obtained in functional assays were comparable to their A_3 AR binding affinity constants, thereby suggesting a receptor-mediated effect. In the light of these results and thanks to their drug-like physicochemical properties, **2a** and **2b** may represent promising lead compounds for the development of adjuvant agents in glioma chemotherapy.

Experimental Section

Chemistry. ^{1}H NMR spectra were recorded on a Varian Gemini 200 spectrometer using DMSO-d_6 as the solvent. IR spectra were recorded with a Pye Unicam Infracord model PU956 in Nujol mulls. Melting points were determined using a Reichert−Köfler hot-stage apparatus and were uncorrected. Thin-layer chromatography (TLC) was performed by using aluminum sheets precoated with silica gel (60 F-254, Merck 0.2 mm), followed by visualization via irradiation with a UV lamp. Flash chromatography was performed using the Flash system (Biotage Corporation). Combustion analyses on target compounds were performed by our Analytical Laboratory in Pisa. All compounds showed ≥95% purity.

The microwave-assisted reactions were performed using a dedicated microwave CEM Discover (CEM Corporation). The wattage was automatically adjusted so as to maintain the desired temperature.

All reagents used were obtained from commercial sources (Sigma-Aldrich). All solvents were of an analytical grade.

The 3-amino-1-methyl-4-pyrazolecarbonitrile **3**,[46] 3-amino-1-benzyl-4-pyrazolecarbonitrile **4**,[27] the 3-amino-1-phenylethyl-4-pyrazolecarbonitrile **5**,[27] and 4-amino-2-benzylpyrazolo[3,4-*d*]pyrimidine **9**[27] were prepared essentially as previously described.

General Procedure for the Synthesis of 4-Amino-2-substituted-6-phenylpyrazolo[3,4-*d*]pyrimidine Derivatives 6−8. A mixture of 3-amino-1-substituted-4-pyrazolecarbonitrile **3**−**5** (10.0 mmol), benzonitrile (1.24 mL, 12.0 mmol), and potassium *tert*-butoxide (0.561 g, 5.00 mmol) was mixed thoroughly and irradiated with microwaves at 150 °C for 3 min. The cooled residue was then diluted with ice−water, and the solid separated was filtered, washed with water, and purified by recrystallization with the appropriate solvent to give the target compounds **6**−**8** (see Supporting Information).

General Procedure for the Synthesis of 6-Phenyl-2-substituted-4-(substituted-aroylamino)pyrazolo[3,4-*d*]pyrimidine Derivatives 2a−c, 2g−i, and 2m−o. A mixture of 4-amino-2-substituted-6-phenylpyrazolo[3,4-*d*]pyrimidine **6**−**8** (10.0 mmol), the suitable aroyl chloride (11.0 mmol), and triethylamine (1.53 mL, 11.0 mmol) was mixed thoroughly and irradiated with microwaves at 110 °C for 5 min. The cooled residue was then diluted with ice−water, and the solid separated was filtered and purified by recrystallization with the appropriate solvent to give target compounds **2a**−**c**, **2g**−**i**, and **2m**−**o** (see Supporting Information).

General Procedure for the Synthesis of 6-Phenyl-2-substituted-4-(substituted-phenylalkylaminocarbamoyl)pyrazolo[3,4-*d*]pyrimidine Derivatives 2d−f, 2j−l, and 2p−r. A mixture of 4-amino-6-phenyl-2-substituted-pyrazolo[3,4-*d*]pyrimidine **6**−**8** (10.0 mmol) and the suitable isocyanate (11.0 mmol) was mixed thoroughly and irradiated with microwaves at 150 °C for 3 min. The cooled residue was then diluted with ice−water, and the solid separated was filtered and purified by recrystallization with the appropriate solvent to give target compounds, **2d**−**f**, **2j**−**l**, and **2p**−**r** (see Supporting Information).

General Procedure for the Synthesis of 2-Benzyl-4-(substituted-aroylamino)pyrazolo[3,4-*d*]pyrimidine derivatives 2s−u. A mixture of 4-amino-2-benzylpyrazolo[3,4-*d*]pyrimidine **9**[27] (10.0 mmol), the suitable aroyl chloride (11.0 mmol), and triethylamine (1.53 mL, 11.0 mmol) was mixed thoroughly and irradiated with microwaves at 110 °C for 5 min. The cooled residue was then diluted with ice−water, and the solid separated was filtered and purified by recrystallization with the appropriate solvent to give target compounds **2s**−**u** (see Supporting Information).

Biological Methods. Materials. [^{3}H]DPCPX, [^{3}H]NECA, and [^{125}I]AB-MECA were obtained from DuPont-NEN (Boston, MA). Adenosine deaminase (ADA) type IX from bovine spleen (150−200 U/mg) and adenosine were from Sigma Chemical Co. (St. Louis, MO). All other reagents were from standard commercial sources and of the highest commercially available grade. CHO cells stably expressing human A_1, A_{2A}, A_{2B}, and A_3 receptors were kindly supplied by Prof. K.-N. Klotz, Wurzburg University, Germany.[47]

Adenosine Receptor Binding Assay. Human A_1 Adenosine Receptors. Aliquots of membranes (30 μg proteins) obtained from A_1 CHO cells were incubated at 25 °C for 180 min in 500 μL of T_1 buffer (50 mM Tris-HCl, 2 mM $MgCl_2$, and 2 units/mL ADA, pH 7.4) containing [^{3}H]DPCPX (3 nM) and six different concentrations of the newly synthesized compounds. Non-specific binding was determined in the presence of 50 μM RPIA.[23] The dissociation constant (K_d) of [^{3}H]DPCPX in A_1 CHO cell membranes was 3 nM.

Human A_{2A} Adenosine Receptors. Aliquots of cell membranes (30 μg) were incubated at 25 °C for 90 min in 500 μL of T_2 buffer (50 mM Tris-HCl, 2 mM $MgCl_2$, and 2 units/mL ADA, pH 7.4) in the presence of 30 nM of [^{3}H]NECA and six different concentrations of the newly synthesized compounds. Non-specific binding was determined in the presence of 100 μM NECA.[23] The dissociation constant (K_d) of [^{3}H]NECA in A_{2A} CHO cell membranes was 30 nM.

Human A_3 Adenosine Receptors. Aliquots of cell membranes (40 μg) were incubated at 25 °C for 90 min in 100 μL of T_3 buffer (50 mM Tris-HCl, 10 mM $MgCl_2$, 1 mM EDTA, and 2 units/mL ADA, pH 7.4) in the presence of 1.4 nM [^{125}I]ABMECA and six different concentrations of the newly synthesized compounds. Non-specific binding was determined in the presence of 50 μM RPIA.[23] The dissociation constant (K_d) of [^{125}I]AB-MECA in A_3 CHO cell membranes was 1.4 nM.

Measurement of Cyclic AMP Levels on hA_{2B} CHO and hA_3 CHO Cells. Intracellular cyclic AMP (cAMP) levels were measured using a competitive protein binding method.[37] CHO cells, expressing recombinant hA_{2B} ARs or hA_3 ARs, were harvested by trypsinization. After centrifugation and resuspension in medium, cells (~48000) were plated in 24-well plates in 0.5 mL of medium. After 48 h, the medium was removed, and the cells were incubated at 37 °C for 15 min with 0.5 mL of DMEM in the presence of adenosine deaminase (1 U/mL) and the phosphodiesterase inhibitor Ro 20-1724 (20 μM). The antagonism profile of the new compounds toward A_{2B} AR was evaluated by assessing their ability to inhibit 100 nM NECA-mediated accumulation of cAMP. The antagonism profile of the new compounds toward A_3 AR was evaluated by assessing their ability to counteract 100 nM NECA-mediated inhibition of cAMP stimulated by 1 μM forskolin. Cells were incubated in the reaction medium (15 min at 37 °C) with different concentrations of the target compound (1 nM to 10 μM) and then were treated with NECA. In parallel, aliquots of cells were treated with the compound alone (10 μM) in the absence or in the presence of forskolin. The reaction was terminated by the removal of the medium and the addition of 0.4 N HCl. After 30 min, lysates were neutralized with 4 N KOH, and the suspension was centrifuged at 800*g* for 5 min. For the determination of cAMP production, bovine adrenal cAMP binding protein was incubated with [^{3}H]cAMP (2 nM) and 50 μL of cell lysate or cAMP standard (0−16 pmol) at 0 °C for 150 min in a total volume of 300 μL. Bound radioactivity was separated by rapid filtration through GF/C glass fiber filters and washed twice with 4 mL 50 mM Tris/HCl, pH 7.4. The

radioactivity was measured by liquid scintillation spectrometry.

All compounds were routinely dissolved in DMSO and diluted with assay buffer to the final concentration with the final amount of DMSO never exceeding 2%. Percent inhibition values for specific radiolabeled ligand binding results at 1−10 μM concentration are means ± SEM of at least three determinations. At least six different concentrations (spanning 3 orders of magnitude) were adjusted appropriately for the IC_{50} of each compound examined. IC_{50} values were computer-generated using a nonlinear regression formula (Graph-Pad, San Diego, CA) and were converted to K_i values using the known K_d values of the radioligands in the different tissues and using the Cheng−Prusoff equation.[48] K_i values were means ± SEM of at least three determinations.

Enzymatic Assay. The activity of the test enzyme was determined spectrophotometrically by monitoring the change in absorbance at 262 nm for 2 min, which was due to the deamination of adenosine catalyzed by ADA. The change in adenosine concentration/min was determined using a Beckman DU-64 kinetics software program (Solf Pack TM module). ADA activity was assayed at 30 °C in a reaction mixture containing 50 μM of adenosine, 50 mM of potassium phosphate buffer, pH = 7.2, and 0.3 nM of enzyme solution in a total volume of 500 μL. The inhibitory activity of the newly synthesized compounds was assayed by adding 100 μL of the inhibitor solution to the reaction mixture described above. All the inhibitors were dissolved in water, and the solubility was facilitated with DMSO, whose concentration never exceeded 4% in the final reaction mixture. To correct for the nonenzymatic changes in adenosine concentration and the absorption values of the test compounds, a reference blank containing all the above assay components except the substrate was prepared. The inhibitory effect of the new derivatives was routinely estimated at a concentration of 10^{-5} M.

Cell Culture and Cell Counting. Cells were grown in culture flasks in RPMI 1640 supplemented with 10% fetal bovine serum (FBS), 100 U/mL penicillin, 100 μg/mL streptomycin, and 2 mM L-glutamine, which were seeded in 24-well plates at densities of 5×10^3 to 1×10^4 cells/well in 500 μL of medium per well. Cells were grown for 24 h in 10% FBS and then were blocked in G1 by reducing the concentration of FBS to 0.5% for 48 h. The medium was changed 2 h prior to treatment, after which cells were treated with the A_3 AR agonist Cl-IB-MECA (100 nM) or IB-MECA (12 nM) in the absence or in the presence of different antagonist concentrations (**2a**: 0.1−10 nM; **2b**: 0.01−5 nM) for 48 h.

At the end of incubation time, living cell counts were determined using the Trypan blue exclusion test.[19,49] Briefly, cells were harvested with trypsin and pooled together with cells floating in the culture medium. An aliquot of this cell suspension was mixed with 0.4% trypan blue in phosphate buffered saline (PBS). Cells were scored on a phase contrast microscope using a Burcke improved counting chamber. Cells with a damaged cell membrane stained blue, while cells that maintained plasma membrane integrity resisted dye entry and remained unstained (apoptotic and healthy cells, respectively).

ERK 1/2 Phosphorylation Assays. A_3 AR-mediated activation of ERK 1/2 phosphorylation in U87MG cells was evaluated by kinetic studies incubating cells with 100 nM Cl-IBMECA for different times (5−120 min). The ERK 1/2 activation was assessed by Fast Activated Cell-Based ELISA kits following the manufacturer's instruction. Following stimulation the cells were rapidly fixed to preserve activation of specific protein modification. Each well was then incubated with primary antibody that recognized phosphorylated ERK 1/2. Subsequent incubation with secondary HRP-conjugated antibody and developing solution allowed a colorimetric quantification of phosphorylated ERK levels. The relative number of cells in each well was then determined using crystal violet solution. The results were calculated by subtracting the mean background from the values obtained from each test condition and were expressed as the percentage of the control (untreated cells).

To evaluate the antagonist profile of the new synthetized compounds on A_3 AR agonist-mediated ERK 1/2 activation, the cells were treated for 30 min with 100 nM Cl-IBMECA in the presence of different **2a** or **2b** compound concentrations. The levels of ERK 1/2 phosphorylation were quantified as above-described.

Modeling Studies. Homology Modeling. The homology model of the hA_3 AR receptor was built using Schrödinger Prime[50] software accessible through the Maestro interface.[51] Unless otherwise stated, default parameters were used throughout. The sequence of the hA_3 AR (P33765) was aligned against the sequence of hA_{2A} AR (P29274). Alignment of anchor residues within each TM domain was attained according to the sequence alignment suggested by Moro and co-workers.[41] During the homology model building, Prime keeps the backbone rigid for the cases in which the backbone does not need to be reconstructed due to gaps in the alignment. The loop refinements were carried out using Prime with default parameter settings, if not mentioned otherwise. Prior to refinement, the protein structures were subjected to a protein preparation step to reorientate side chain hydroxyl groups and alleviate potential steric clashes. The implemented loop modeling protocol consists of several steps.[52] First, large numbers of loops are created by a conformational search in dihedral angle space. Clustering of loop conformations and side chain optimization is performed to select representative solutions. On the basis of the user parameters, a limited number of structures is then processed using complete energy minimization. The top ranked solution in terms of Prime energy is considered best. The short loops (ELI and ELIII) were refined using default sampling rates in the initial step, while the extended highest sampling rate was chosen for the larger amino acid loops (ELII). Side chains were unfrozen within 7.5 Å of the corresponding loop, and the energy cutoff was set to 10 kcal.

AD4 Docking Calculations. The new version of the docking program AutoDock (version 4, AD4),[53] as implemented through the graphical user interface called AutoDockTools (ADT), was used to dock **2b**, **2i**, **2o**, and **2u**. Ligand structures were built using the builder in the Maestro package of Schroedinger Suite 2007 and optimized using a version of MacroModel also included. The constructed compounds and the receptor structure were converted to AD4 format files using ADT generating automatically all other atom values. The docking area was centered around the putative binding site. A set of grids of 60 Å × 60 Å × 60 Å with 0.375 Å spacing was calculated around the docking area for the ligand atom types using AutoGrid4. For each ligand, 100 separate docking calculations were performed. Each docking calculation consisted of 10 million energy evaluations using the Lamarckian genetic algorithm local search (GALS) method. The GALS method evaluates a population of possible docking solutions and propagates the most successful individuals from each generation into the subsequent generation of possible solutions. A low-frequency local search according to the method of Solis and Wets is applied to docking trials to ensure that the final solution represents a local minimum. All dockings described in this paper were performed with a population size of 250, and 300 rounds of Solis and Wets local search were applied with a probability of 0.06. A mutation rate of 0.02 and a crossover rate of 0.8 were used to generate new docking trials for subsequent generations, and the best individual from each generation was propagated over the next generation. The docking results from each of the 100 calculations were clustered on the basis of root-mean square deviation (rmsd) (solutions differing by less than 2.0 Å) between the Cartesian coordinates of the atoms and were ranked on the basis of free energy of binding (ΔG_{AD4}). The top-ranked compounds were visually inspected for good chemical geometry. Because AD4 does not perform any structural optimization and

energy minimization of the complexes found, a molecular mechanics/energy minimization (MM/EM) approach was applied to refine the AD4 output. The computational protocol applied consisted of the application of 100000 steps of the Polak−Ribiére conjugate gradients (PRCG) or until the derivative convergence was 0.05 kJ/mol. All complexes pictures were rendered employing the UCSF Chimera software.[54]

Acknowledgment. This work was financially supported by MIUR (ex 40%). We thank Prof. Dr. Karl-Norbert Klotz for his generous gift of transfected CHO cells expressing human A_1, A_{2A}, A_{2B}, and A_3 adenosine receptors.

Supporting Information Available: Physical properties and spectral data of compounds **6**−**8** and **2a**−**u**, and analytical data of compounds **6**−**8** and **2a**−**u**. This material is available free of charge via the Internet at http://pubs.acs.org.

References

(1) Poulsen, S.-A.; Quinn, R. J. Adenosine receptors: new opportunities for future drugs. *Bioorg. Med. Chem.* **1998**, *6*, 619–641.
(2) Fredholm, B. B.; Arslan, G.; Halldner, L.; Kull, B.; Schulte, G.; Wasserman, W. Structure and function of adenosine receptors and their genes. *Naunyn-Schmiedeberg's Arch. Pharmacol.* **2000**, *362*, 364–374.
(3) Fredholm, B. B.; IJzerman, A. P.; Jacobson, K. A.; Klotz, K.-N.; Linden, J. International Union of Pharmacology. XXV. Nomenclature and classification of adenosine receptors. *Pharmacol. Rev.* **2001**, *53*, 527–552.
(4) Schulte, G.; Fredholm, B. B. Signalling from adenosine receptors to mitogen-activated protein kinases. *Cell. Signalling* **2003**, *15*, 813–827.
(5) Jacobson, K. A.; Gao, Z.-G. Adenosine receptors as therapeutic targets. *Nat. Rev. Drug Discovery* **2006**, *5*, 247–264.
(6) Moro, S.; Gao, Z.-G.; Jacobson, K. A.; Spalluto, G. Progress in the pursuit of therapeutic adenosine receptor antagonists. *Med. Res. Rev.* **2006**, *26*, 131–159.
(7) Linden, J.; Taylor, H. E.; Robeva, A. S.; Tucker, A. L.; Stehle, J. H.; Rivkees, S. A.; Fink, J. S.; Reppert, S. M. Molecular Cloning and Functional Expression of a Sheep A_3 Adenosine Receptor with Widespread Tissue Distribution. *Mol. Pharmacol.* **1993**, *44*, 524–532.
(8) Linden, J. Cloned adenosine A_3 receptors: pharmacological properties, species differences and receptor functions. *Trends Pharmacol. Sci.* **1994**, *15*, 298–306.
(9) Liang, B. T.; Jacobson, K. A. A physiological role of the adenosine A_3 receptor: sustained cardioprotection. *Proc. Natl. Acad. Sci. U.S. A.* **1998**, *95*, 6995–6999.
(10) Headrick, J. P.; Peart, J. A_3 adenosine receptor-mediated protection of the ischemic heart. *Vasc. Pharmacol.* **2005**, *42*, 271–279.
(11) Akkari, R.; Burbiel, J. C.; Hockemeyer, J.; Müller, C. E. Recent Progress in the Development of Adenosine Receptor Ligands as Antiinflammatory Drugs. *Curr. Top. Med. Chem.* **2006**, *6*, 1375–1399.
(12) Mitchell, C. H.; Peterson-Yantorno, K.; Carre, D. A.; McGlinn, A. M.; Coca-Prados, M.; Stone, R. A.; Civan, M. M. A_3 adenosine receptors regulate Cl^- channels of nonpigmented ciliary epithelial cells. *Am. J. Physiol.* **1999**, *276*, 659–666.
(13) Brambilla, R.; Cattabeni, F.; Ceruti, S.; Barbieri, D.; Franceschi, C.; Kim, Y.-C.; Jacobson, K. A.; Klotz, K.-N.; Lohse, M. J.; Abbracchio, M. P. Activation of the A_3 adenosine receptor affects cell cycle progression and cell growth. *Naunyn-Schmiedeberg's Arch. Pharmacol.* **2000**, *361*, 225–234.
(14) Baraldi, P. G.; Tabrizi, M. A.; Romagnoli, R.; Fruttarolo, F.; Merighi, S.; Varani, K.; Gessi, S.; Borea, P. A. Pyrazolo[4,3-*e*]1,2,4-triazolo[1,5-*c*]pyrimidine Ligands, New Tools to Characterize A_3 Adenosine Receptors in Human Tumor Cell Lines. *Curr. Med. Chem.* **2005**, *12*, 1319–1329.
(15) Gessi, S.; Cattabriga, E.; Avitabile, A.; Gafà, R.; Lanza, G.; Cavazzini, L.; Bianchi, N.; Gambari, R.; Feo, C.; Liboni, A.; Gullini, S.; Leung, E.; Mac-Lennan, S.; Borea, P. A. Elevated Expression of A_3 Adenosine Receptors in Human Colorectal Cancer is Reflected in Peripheral Blood Cells. *Clin. Cancer Res.* **2004**, *10*, 5895–5901.
(16) Fishman, P.; Bar-Yehuda, S. Pharmacology and Therapeutic Applications of A_3 Receptor Subtype. *Curr. Top. Med. Chem.* **2003**, *3*, 463–469.
(17) Gessi, G.; Merighi, S.; Varani, K.; Cattabriga, E.; Benini, A.; Mirandola, P.; Leung, E.; Mac Lennan, S.; Feo, C.; Baraldi, S.; Borea, P. A. Adenosine Receptors in Colon Carcinoma Tissues and Colon Tumoral Cell Lines: Focus on the A_3 Adenosine Subtype. *J. Cell. Physiol.* **2007**, *211*, 826–836.
(18) Merighi, S.; Mirandola, P.; Varani, K.; Gessi, S.; Capitani, S.; Leung, E.; Baraldi, P. G.; Tabrizi, M. A.; Borea, P. A. Pyrazolotriazolopyrimidine derivatives sensitive melanoma cells to the chemiotherapic drugs: taxol and vindesine. *Biochem. Pharmacol.* **2003**, *66*, 739–748.
(19) Morrone, F. B.; Jacques-Silva, M. C.; Horn, A. P.; Bernardi, F.; Schwartsmann, G.; Rodnight, R.; Lenz, G. Extracellular nucleotides and nucleosides induce proliferation and increase nucleoside transport in human glioma cell lines. *J. Neuro-Oncol.* **2003**, *64*, 211–218.
(20) Merighi, S.; Benini, A.; Mirandola, P.; Gessi, S.; Varani, K.; Leung, E.; Maclennan, S.; Borea, P. A. Adenosine modulates vascular endothelial growth factor expression via hypoxia-inducible factor-1 in human glioblastoma cells. *Biochem. Pharmacol.* **2006**, *72*, 19–31.
(21) Da Settimo, F.; Primofiore, G.; Taliani, S.; Marini, A. M.; La Motta, C.; Novellino, E.; Greco, G.; Lavecchia, A; Trincavelli, M. L.; Martini, C. 3-Aryl[1,2,4]triazino[4,3-*a*]benzimidazol-4(10*H*)-ones: a new class of selective A_1 adenosine receptor antagonists. *J. Med. Chem.* **2001**, *44*, 316–327.
(22) Novellino, E.; Abignente, E.; Cosimelli, B.; Greco, G.; Iadanza, M.; Laneri, S.; Lavecchia, A.; Rimoli, M. G.; Da Settimo, F.; Primofiore, G.; Tuscano, D.; Trincavelli, L.; Martini, C. Design, synthesis and biological evaluation of novel *N*-alkyl- and *N*-acyl-(7-substituted-2-phenylimidazo[1,2-*a*][1,3,5]triazin-4-yl]amines (ITAs) as novel A_1 adenosine receptor antagonists. *J. Med. Chem.* **2002**, *45*, 5030–5036.
(23) Da Settimo, F.; Primofiore, G.; Taliani, S.; La Motta, C.; Novellino, E.; Greco, G.; Lavecchia, A.; Cosimelli, B.; Iadanza, M.; Klotz, K.-N.; Tuscano, D.; Trincavelli, M. L.; Martini, C. A_1 Adenosine receptor antagonists, 3-aryl[1,2,4]triazinobenzimidazol-4-(10*H*)-ones (ATBIs) and *N*-alkyl and *N*-acyl-(7-substituted-2-phenylimidazo[1,2-*a*][1,3,5]triazin-4-yl)amines (ITAs): different recognition of bovine and human binding sites. *Drug Dev. Res.* **2004**, *63*, 1–7.
(24) Novellino, E.; Cosimelli, B.; Ehlardo, M.; Greco, G.; Iadanza, M.; Lavecchia, A.; Rimoli, M. G.; Sala, A.; Da Settimo, A.; Primofiore, G.; Da Settimo, F.; Taliani, S.; La Motta, C.; Klotz, K.-N.; Tuscano, D.; Trincavelli, M. L.; Martini, C. 2-(Benzimidazol-2-yl)quinoxalines: A Novel Class of Selective Antagonists at Human A_1 and A_3 Adenosine Receptors Designed by 3D Database Searching. *J. Med. Chem.* **2005**, *48*, 8253–8260.
(25) Da Settimo, F.; Primofiore, G.; Taliani, S.; Marini, A. M.; La Motta, C.; Simorini, F.; Salerno, S.; Sergianni, V.; Tuccinardi, T.; Martinelli, A.; Cosimelli, B.; Greco, G.; Novellino, E.; Ciampi, O.; Trincavelli, M. L.; Martini, C. 5-Amino-2-phenyl[1,2,3]triazolo-[1,2-*a*][1,2,4]benzotriazin-1-one: A Versatile Scaffold To Obtain Potent and Selective A_3 Adenosine Receptor Antagonists. *J. Med. Chem.* **2007**, *50*, 5676–5684.
(26) Cosimelli, B.; Greco, G.; Ehlardo, M.; Novellino, E.; Da Settimo, F.; Taliani, S.; La Motta, C.; Bellandi, M.; Tuccinardi, T.; Martinelli, A.; Ciampi, O.; Trincavelli, M. L.; Martini, C. Derivatives of 4-Amino-6-hydroxy-2-mercaptopyrimidine as Novel, Potent, and Selective A_3 Adenosine Receptor Antagonists. *J. Med. Chem.* **2008**, *51*, 1764–1770.
(27) Da Settimo, F.; Primofiore, G.; La Motta, C.; Taliani, S.; Simorini, F.; Marini, A. M.; Mugnaini, L.; Lavecchia, A.; Novellino, E.; Tuscano, D.; Martini, C. Novel, Highly Potent Adenosine Deaminase Inhibitors Containing the Pyrazolo[3,4-*d*]pyrimidine Ring System. Synthesis, Structure−Activity Relationships, and Molecola Modeling Studies. *J. Med. Chem.* **2005**, *48*, 5162–5174.
(28) Antonioli, L.; Fornai, M.; Colucci, R.; Ghisu, N.; Da Settimo, F.; Natale, G.; Kastsiuchenka, O.; Duranti, E.; Virdis, A.; Vassalle, C.; La Motta, C.; Mugnaini, L.; Breschi, M. C.; Blandizzi, C.; Del Tacca, M. Inhibition of Adenosine Deaminase Attenuates Inflammation in Experimental Colitis. *J. Pharmacol. Exp. Ther.* **2007**, *322*, 435–442.
(29) Chebib, M.; Quinn, R. J. Pyrazolo[3,4-*d*]pyrimidines; Adenosine Receptor Selectivity. *Bioorg. Med. Chem. Lett.* **1995**, *5*, 2409–2412.
(30) Chebib, M.; Quinn, R. J. 1-Phenylpyrazolo[3,4-*d*]pyrimidines as Adenosine Antagonists: The Effects of Substituents at C4 and C6. *Bioorg. Med. Chem.* **1997**, *5*, 311–322.
(31) Briel, D.; Aurich, R.; Egerland, U.; Unverferth, K. Synthesis of substituted 6-phenylpyrazolo[3,4-*d*]pyrimidines with potential adenosin-A_{2A} antagonistic activity. *Pharmazie* **2005**, *60*, 732–735.
(32) Kim, Y.-C.; Ji, X.-D.; Jacobson, K. A. Derivatives of the Triazoloquinazoline Adenosine Antagonist (CGS 15943) Are Selective

for the Human A_3 Receptor Subtypes. *J. Med. Chem.* **1996**, *39*, 4142–4148.
(33) Baraldi, P. G.; Cacciari, B.; Romagnoli, R.; Merighi, S.; Varani, K.; Borea, P. A.; Spalluto, G. A_3 Adenosine Receptor Ligands: History and Perspectives. *Med. Res. Rev.* **2000**, *20*, 103–128.
(34) Baraldi, P. G.; Cacciari, B.; Borea, P. A.; Varani, K.; Pastorin, G.; Da Ros, T.; Tabrizi, M. A.; Fruttarolo, F.; Spalluto, G. Pyrazolo-Triazolo-Pyrimidine Derivatives as Adenosine Receptor Antagonists: A Possible Template for Adenosine Receptor Subtypes? *Curr. Pharm. Des.* **2002**, *8*, 2299–2332.
(35) Van Muijlwijk-Koezen, J. E.; Timmerman, H.; Link, R.; van der Goot, H.; IJzerman, A. P. A Novel Class of Adenosine A_3 Receptor Ligands. 2. Structure−Affinity Profile of a Series of Isoquinoline and Quinazoline Compounds. *J. Med. Chem.* **1998**, *41*, 3994–4000.
(36) Lenzi, O.; Colotta, V.; Catarzi, D.; Varano, F.; Filacchioni, G.; Martini, C.; Trincavelli, L.; Ciampi, O.; Varani, K.; Marighetti, F.; Morizzo, E.; Moro, S. 4-Amido-2-aryl-1,2,4-triazolo[4,3-*a*]quinoxalin-1-ones as new potent and selective human A_3 adenosine receptor antagonists. Synthesis, pharmacological evaluation, and ligand-receptor modeling studies. *J. Med. Chem.* **2006**, *49*, 3916–3925.
(37) Nordstedt, C.; Fredholm, B. B. A modification of a protein-binding method for rapid quantification of cAMP in cell-culture supernatants and body fluid. *Anal. Biochem.* **1990**, *189*, 231–234.
(38) Beukers, M. W.; Chang, L. C. W.; von Frijtag Drabbe Kunzel, J. K; Mulder-Krieger, T.; Spanjersberg, R. F.; Brussee, J.; IJzerman, A. P. New, non-adenosine, high-potency agonists for the human adenosine A_{2B} receptor with an improved selectivity profile compared to the reference agonist *N*-ethylcarboxamidoadenosine. *J. Med. Chem.* **2004**, *47*, 3707–3709.
(39) Chang, L. C. W.; von Frijtag Drabbe Kunzel, J. K.; Mulder-Krieger, T.; Spanjersberg, R. F.; Roerink, S. F.; van den Hout, G.; Beukers, M. W.; Brussee, J.; IJzerman, A. P. A series of ligands displaying a remarkable agonistic−antagonistic profile at the adenosine A_1 receptor. *J. Med. Chem.* **2005**, *48*, 2045–2053.
(40) Jaakola, V. P.; Griffith, M. T.; Hanson, M. A.; Cherezov, V.; Chien, E. Y. T.; Lane, J. R.; IJzerman, A. P.; Stevens, R. C. The 2.6 angstrom crystal structure of a human A_{2A} adenosine receptor bound to an antagonist. *Science* **2008**, *322*, 1211–1217.
(41) Lenzi, O.; Colotta, V.; Catarzi, D.; Varano, F.; Poli, D.; Filacchioni, G.; Varani, K.; Vincenzi, F.; Borea, P. A.; Paoletta, S.; Morizzo, E.; Moro, S. 2-Phenylpyrazolo[4,3-*d*]pyrimidin-7-one as a New Scaffold To Obtain Potent and Selective Human A_3 Adenosine Receptor Antagonists: New Insights into the Receptor-Antagonist Recognition. *J. Med. Chem.* **2009**, *52*, 7640–7652.
(42) Huey, R.; Morris, G. M.; Olson, A. J.; Goodsell, D. S. A Semiempirical Free Energy Force Field with Charge-Based Desolvation. *J. Comput. Chem.* **2007**, *28*, 1145–1152.
(43) Kim, J.; Wess, J.; van Rhee, M.; Schoneberg, T.; Jacobson, K. A. Site-directed mutagenesis identifies residues involved in ligand recognition in the human A_{2A} adenosine receptor. *J. Biol. Chem.* **1995**, *270*, 13987–13997.
(44) Gao, Z.-G.; Chen, A.; Barak, D.; Kim, S.-K.; Muller, C. E.; Jacobson, K. A. Identification by site-directed mutagenesis of residues involved in ligand recognition and activation of the human A_3 adenosine receptor. *J. Biol. Chem.* **2002**, *277*, 19056–19063.
(45) The CLogP, ASA, and TPSA calculations were performed with the Marvin Sketch and Calculator Plugins on the website http://www.chemaxon.com/demosite/marvin/index.html.
(46) Baraldi, P. G.; Borea, P. A. Preparation of pyrazolo[4,3-*e*]1,2,4-triazolo[1,5-*c*]pyrimidines and analogs as adenosine A_3 receptor modulators for therapeutic and diagnostic use. U.S. Patent Appl. US6407236 B1 20020618, 2002.
(47) Klotz, K.-N.; Hessling, J.; Hegler, J.; Owman, C.; Kull, B.; Fredholm, B. B.; Lohse, M. J. Comparative pharmacology of human adenosine receptor subtypes characterization of stably transfected receptors in CHO cells. *Naunyn-Schmiedebergs Arch. Pharmacol.* **1998**, *357*, 1–9.
(48) Cheng, Y. C.; Prusoff, W. H. Relation between the inhibition constant K_i and the concentration of inhibitor which causes fifty percent inhibition (IC_{50}) of an enzymatic reaction. *Biochem. Pharmacol.* **1973**, *22*, 3099–3108.
(49) Bjorklund, O.; Shang, M.; Tonazzini, I.; Darè, E.; Fredholm, B. B. Adenosine A_1 and A_3 receptors protect astrocytes from hypoxic damage. *Eur. J. Pharmacol.* **2008**, *596*, 6–13.
(50) *Prime, version 2.0*; Schrödinger, LLC, New York, **2005**.
(51) *Maestro, version 8.5*; Schrödinger, LLC, New York, **2006**.
(52) Jacobson, M. P.; Pincus, D. L.; Rapp, C. S.; Day, T. J.; Honig, B.; Shaw, D. E.; Friesner, R. A. A hierarchical approach to all-atom protein loop prediction. *Proteins* **2004**, *55*, 351–367.
(53) Huey, R.; Morris, G. M.; Olson, A. J.; Goodsell, D. S. A Semiempirical Free Energy Force Field with Charge-Based Desolvation. *J. Comput. Chem.* **2007**, *28*, 1145–1152.
(54) Pettersen, E. F.; Goddard, T. D.; Huang, C. C.; Couch, G. S.; Greenblatt, D. M.; Meng, E. C.; Ferrin, T. E. UCSF Chimera—A Visualization System for Exploratory Research and Analysis. *J. Comput. Chem.* **2004**, *25*, 1605–1612.